

## Article

# Study on Secondary Brine Drainage and Sand Control Technology of Salt Cavern Gas Storage

Yi Zhang <sup>1</sup>, Kun Zhang <sup>2</sup>, Jun Li <sup>1</sup>, Yang Luo <sup>3</sup>, Li-Na Ran <sup>1</sup>, Lian-Qi Sheng <sup>2</sup> and Er-Dong Yao <sup>2,\*</sup> 

<sup>1</sup> PetroChina Research Institute of Petroleum Exploration & Development, Beijing 100083, China

<sup>2</sup> State Key Laboratory of Petroleum Resources and Prospecting, China University of Petroleum, Beijing 102249, China

<sup>3</sup> Shixi Field Operation District, PetroChina, Xinjiang Oilfield Company, Karamay 834000, China

\* Correspondence: yaoed@cup.edu.cn

**Abstract:** Geological conditions of salt cavern gas storage in China are characterized by dominantly layered salt layers with a high content of insoluble mudstone. After the water leaching of the salt layer, a large amount of sediment accumulates at the bottom of the gas storage cavity. During the gas injection process, only the clean brine above the sediment can be expelled, leaving a brine layer of 2–5 m and a large amount of brine in the pore space of the sediment. To increase storage capacity, it is urgent to explore the secondary gas injection and brine drainage technology to further expel residual brine in pores of the sediment at the cavern bottom. The sediment is relatively loosely packed and is composed of mudstone particles, which easily migrate and block the brine withdrawal pipe. In this paper, firstly, the mineral composition, particle size and distribution characteristics of the sediment at the bottom of the salt cavern are fully understood by XRD and sieve analysis methods. Then, a lab simulation device suitable for secondary gas injection and brine drainage of a high-salinity salt cavern with a diameter and height of 25 cm was designed and built. A screen sand control experiment, a gravel pack artificial wall sand control experiment and chemical cementing sand were simulated. The effects of gas injection, brine drainage pressure, brine layer height and insoluble particle size on sand production and liquid drainage were studied. The influence factors of brine withdrawal on the sand control in secondary brine drainage were intensively investigated, and finally, the gravel pack artificial wall sand control technology system was recommended. The optimal construction parameters for secondary brine discharge are recommended as follows: Under the condition of gravel packing with the same particle size, the trend of sand content with different artificial wall thicknesses is not obvious, and a 2 cm wall thickness is the best in the overall experiment, corresponding to 28 cm in the field. The larger the particle size of the gravel pack, the better the sand control, and the best gravel size is 10–20 mesh. The injection pressure should be as low as possible.

**Keywords:** secondary brine discharge; sediment control; salt cavern gas storage



**Citation:** Zhang, Y.; Zhang, K.; Li, J.; Luo, Y.; Ran, L.-N.; Sheng, L.-Q.; Yao, E.-D. Study on Secondary Brine Drainage and Sand Control Technology of Salt Cavern Gas Storage. *Sustainability* **2023**, *15*, 7793. <https://doi.org/10.3390/su15107793>

Academic Editors: Kaihui Li and Jianjun Ma

Received: 23 February 2023

Revised: 4 May 2023

Accepted: 8 May 2023

Published: 10 May 2023



**Copyright:** © 2023 by the authors. Licensee MDPI, Basel, Switzerland. This article is an open access article distributed under the terms and conditions of the Creative Commons Attribution (CC BY) license (<https://creativecommons.org/licenses/by/4.0/>).

## 1. Introduction

Natural gas is an efficient, environmentally friendly and clean energy. The demand for natural gas in China is growing, and the proportion of natural gas consumption is gradually increasing. However, there is still great potential for the storage of natural gas in China [1,2]. Salt cavern gas storage has great advantages in the storage of natural gas, as it has less ground occupation, it is conducive to fire prevention and pollution prevention and its injection–production conversion is very fast. Developing salt cavern gas storage has become an effective way to store natural gas [3,4].

Generally, thick salt layers or salt domes are used in the construction of salt cavern gas storage. Clean water is injected through the pipe in an artificial way to dissolve the salt layer. The cave formed by water leaching is the gas storage [5,6]. In the process of cavity formation of dissolved salt, thermal–elastoplastic changes are generated due to internal

temperature, pressure, etc., and a well-sealed cavity is finally formed, with good stability and air storage ability [7–9]. Salt cavern gas storage in Europe and the United States has good geological conditions, a high salt content of the salt dome and low mud content, resulting in a simple construction operation [10]. However, the geological conditions of salt cavern gas storage in China all contain a large number of salt layers with thin thicknesses (about 150 m). A large number of insoluble argillaceous interlayers (15–40%) exist in the salt layers with a large thickness (3–11 m) [11]. After the water-leaching process, the insoluble interlayers in the salt layers lose their support, gradually collapse and settle and finally accumulate at the bottom of the gas storage cavity. The insoluble mudstones are released and accumulated by free settling, and their arrangement is loose. These insoluble sediments have abundant pore space between the particles, which is occupied by the saturated brine. What is more, parts of the clay minerals swell and increase in volume [12,13]. The transport characteristics of salt cavern gas storage largely depend on the permeability of insoluble particles at the bottom [14,15]. Therefore, brine in the pores occupies considerable space for gas storage. In the process of the first gas injection, only the clean brine above the sediment can be expelled and leave the 2–5 m brine layer and the brine in the pore space [16]. China's salt cavern gas storage has the problem that insoluble residue occupies a large amount of storage capacity. To solve this problem and expand storage capacity, the remaining brine should be expelled. Therefore, it is necessary to carry out secondary gas injection to expel brine. In this process, it is necessary to consider how to filter insoluble particles to prevent sand production [8,17]. At the same time, the permeability of insoluble residue will not decrease on the basis of halogen discharge sand control [18,19].

Several research groups have conducted theoretical research and scientific interpretation of the particle size, porosity and particle settling pattern at the bottom of the gas storage cavity. They try to understand the characteristics of the sediment and explore the feasibility of secondary gas injection and brine withdrawal [20]. This paper mainly aims to evaluate the adaptability of conventional mechanical sand control, gravel filling and artificial well wall sand control technologies. The sand control effects of the three technologies were compared for uncemented rock particles, and the best technology was optimized on this basis. The new technology will further expel the remaining brine and brine in the pore of the uncemented sediments to increase the storage capacity. The final results are as follows: Under the condition of gravel packing with the same particle size, the trend of sand content with different artificial wall thicknesses is not obvious, and a 2 cm wall thickness is the best in the overall experiment, corresponding to 28 cm in the field. The larger the particle size of the gravel pack, the better the sand control, and the best gravel size is 10–20 mesh. Compared with other methods, this method has a better sand control effect and a lower sand production rate for uncemented sediments.

## 2. Analysis of Reservoir and Sediment Characteristics

### 2.1. Mineral Analysis of the Sediment from Cavern Bottom

#### 2.1.1. Experimental Material

The target block of this paper is the Chuzhou salt cavern gas storage, located in Huai'an City, Jiangsu Province [21]. The strata in this area are successively divided into the Dongtai Formation of the Quaternary System, Neogene salt formation and Cretaceous Pukou Formation from top to bottom. The strata of the target salt cavern gas storage are the upper salt layer of the second Pukou Formation, and the salt layer distribution is stable. Through the whole rock mineral composition analysis of the sample rock cores, the mineral composition type and content of the target gas storage can be obtained, which provides a solid experimental basis for the subsequent sand control technology [22].

The mineral analysis of salt cavern gas storage is carried out by using an X-ray diffractometer (XRD). Rietveld refinement of crystal structures is performed by using powder X-ray diffraction data [23]. The method has no damage to the sample, no pollution and high measurement accuracy, so it is widely used in mineral composition analysis

experiments [12]. The experimental samples were taken from the CZ2 and CZ3 wells and provided by the target salt cavern gas storage site [24].

### 2.1.2. Experimental Results

Four groups of CZ2 core samples and four groups of CZ3 core samples were tested through XRD diffraction (Figure 1). Since there was not much difference in the mineral composition and content of salt rock samples, they could be combined to calculate the average value. The results are shown in Tables 1 and 2 below [25].



**Figure 1.** Diagram of CZ-2 core and powder.

**Table 1.** Analysis of mineral composition and content in Block CZ (Unit: wt.%).

Sample	Pl	Qtz	Mic	Cal	Dol	Py	Gp	Clay Mineral
CZ2-1	25	23	8	21	5	4	8	6
CZ2-2	28	17	10	7	10	-	21	7
CZ2-3	21	5	2	4	3	5	38	23
CZ2-4	36	21	12	-	18	4	4	6
CZ3-1	39	16	5	5	24	5	1	5
CZ3-2	28	26	10	12	13	5	-	6
CZ3-3	25	29	22	11	7	7	4	5
CZ3-4	36	32	4	11	6	1	3	7
Average value	30	22	8	9	11	4	8	8

Note: Pl is Plagioclase, Qtz is Quartz, Mi is Mic, Cal is Calcite, Dol is Dolomite, Py is Pyrite and Gp is Gypsum.

**Table 2.** Analysis of clay minerals in Block CZ.

Sample	Relative Clay Mineral Content (%)					Mixed-Layer Ratio		
	S	I/S	It	Kao	C	C/S	I/S	C/S
CZ2-1	-	16	39	2	10	33	10	40
CZ2-2	-	20	40	3	12	25	10	40
CZ2-3	-	45	40	-	15	-	75	-
CZ2-4	-	13	47	-	14	26	35	50
CZ3-1	-	13	49	-	14	24	10	25
CZ3-2	-	10	48	4	7	31	10	40
CZ3-3	-	12	40	3	6	39	10	40
CZ3-4	-	20	38	3	6	33	10	40
Average value	-	19	43	2	10	26	21	34

Note: S is montmorillonite, It is illite, Kao is kaolinite and C is chlorite.

As can be seen from Figure 2, Tables 1 and 2, plagioclase is the most abundant mineral at the bottom of the salt cavern, accounting for about 30%; quartz is the second most abundant mineral, accounting for about 22%; and the content of other minerals is relatively small—mica is about 8%, calcite is about 9% and dolomite is about 11%. The remaining clay content is about 8%. Due to the saturated brine remaining in the bottom of the cavity, the brine has a great impact on the swelling rate of different clay minerals, so it is necessary to conduct a detailed analysis of clay minerals. As can be seen from Table 2, illite is the dominant clay mineral followed by chlorite, accounting for 10%, and others are mostly

mixed layers of different clay minerals. The hydration expansion of montmorillonite, particle migration of illite and acid sensitization of chlorite occurred. According to the clay analysis results, the content of montmorillonite is low, and it is easily swelling clay. Therefore, the clay hydration will not occur apparently in the sediment at the bottom of the cavity [26].

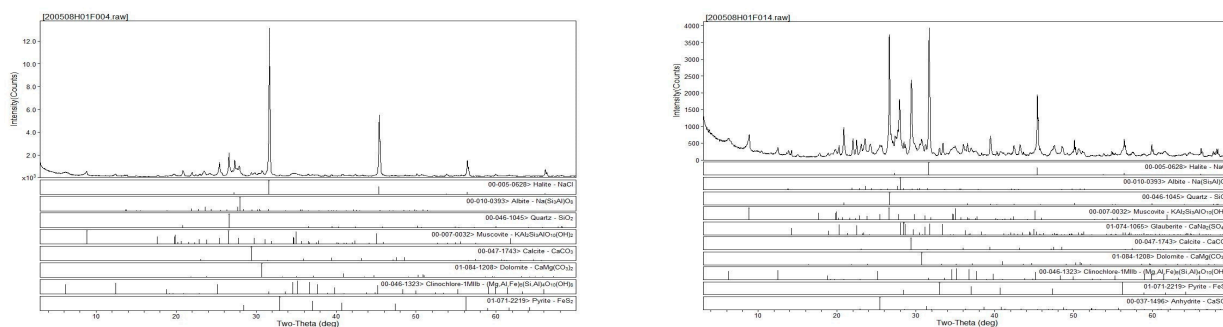


Figure 2. Mineral analysis spectra.

## 2.2. Particle Size Distribution of the Insoluble Sediment

At present, there are many methods to determine the particle size of rocks and minerals. Among them, the simplest and most widely used is the screening method, which can not only measure the particle size distribution but also draw the cumulative particle size distribution curve through the measured data so as to analyze the particle size distribution of the samples [27]. In this experiment, the sieving method was used to determine the particle size distribution of the sediment at the bottom of the cavity, and the experimental results are shown in Table 3 and Figure 3. Figure 4 shows the gain size distribution curve after the mesh number is converted to particle size.

Table 3. Particle size distribution of the insoluble sediment.

Sieve Mesh	Particle Diameter (mm)	Number Sieve Mass (g)	Grading Mass Fraction (%)	Above Sieve Mass Fraction (%)	Below Sieve Mass Fraction (%)
4	6.00	7.44	1.73	1.73	100.00
5	5.00	33.36	7.74	9.47	97.67
6	4.00	113.59	26.37	35.84	91.75
7	3.50	12.74	2.96	38.80	65.67
8	3.00	67.35	15.64	54.44	69.97
12	1.60	55.43	12.87	67.30	46.48
20	1.00	43.28	10.05	77.35	33.17
40	0.45	24.03	5.58	82.93	21.79
50	0.36	25.61	5.95	88.88	17.57
80	0.20	18.92	4.39	93.27	12.34
120	0.12	22.11	5.13	98.40	6.73
200	0.07	6.36	1.48	99.88	1.53
300	0.05	0.52	0.12	100.00	0.12

According to the data shown in Table 3, mass fraction curves of particle size are drawn, as shown in Figure 3. As can be seen from Figure 3 and Table 3, the particle size distribution of the sediment ranges from 0.005 mm to 5 mm, and the corresponding mesh number ranges from 3 mesh to 400 mesh. The particle size distribution is divided into six ranges: <0.25 mm, 0.25 mm~0.5 mm, 0.5 mm~1 mm, 1 mm~2 mm, 2 mm~3 mm and >3 mm. The mass percentage of each range was 32.7%, 12.87%, 15.64%, 2.96%, 26.37% and 9.47%, respectively. The mass fraction of the sediment in the range of <0.25 mm and 2 mm~3 mm is the largest, and the proportion is 32.7%. It indicates that the particle size of the sediment at the bottom of the salt cave has a bimodal distribution, and there are two types of particle

sizes: large and small. Since most of the particles in the sediment are larger than 0.25 mm in size, there are many space gaps between these particles, which could also be used as the storage space of natural gas. The purpose of this paper is to expel the brine in these pores and to increase the storage space of the gas storage as much as possible [28].

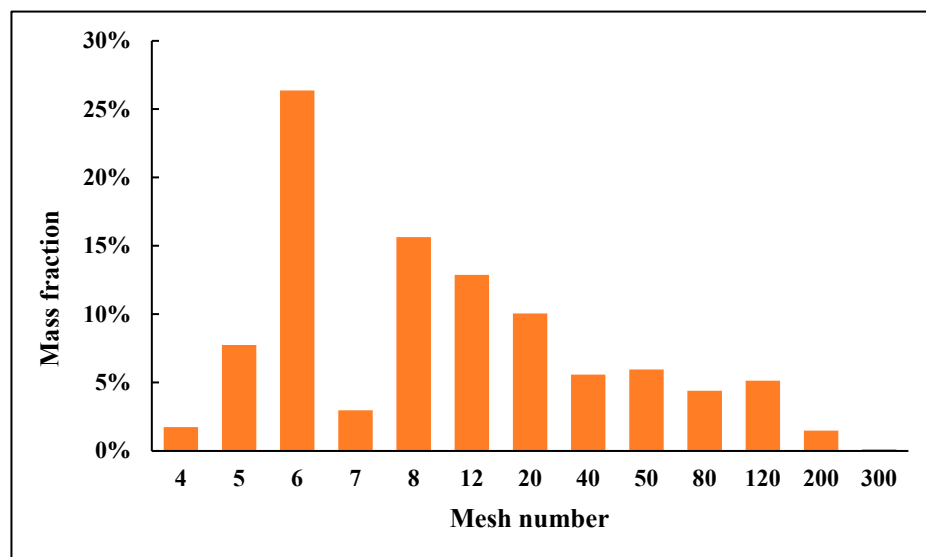


Figure 3. Mass fraction of accumulation particle size classification.

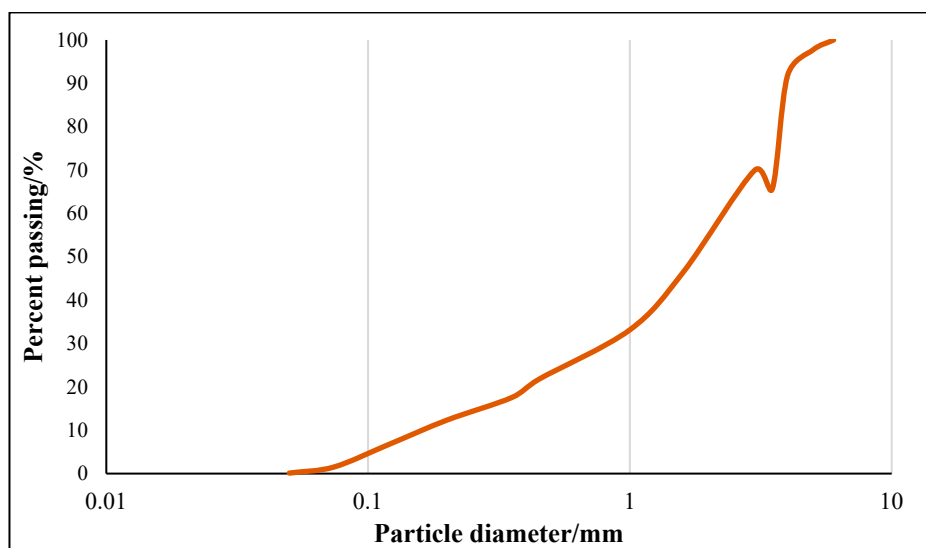


Figure 4. The gain size distribution curve.

### 3. Experiment and Device Design of Secondary Gas Injection for Brine Drainage

Gas injection and brine drainage is the last step in the construction of salt cavern gas storage. High pressure is used to inject natural gas through pipelines from the ground. When the gas injection pressure is greater than the pressure in the gas storage chamber, the brine in the chamber is expelled from the brine drainage pipe [29]. In the leaching process of the cavern, the insoluble mud interlayer collapses and settles at the bottom to form loose sediment, which cannot be carried to the ground with the movement of brine. According to the sonar data of salt cavern gas storage, the volume of settling residues at the bottom accounts for 45% of the volume of the salt cavern. The thickness of the remaining brine layer above the residues is about 2~5 m. In order to expel the brine in the cavity as much as possible, it is necessary to increase the depth of the brine drainage pipe [30,31].

When the brine-expelled string is located above the sediment at the bottom of the cavern, it is normal brine withdrawal, which is called primary brine drainage in this paper. When the bottom of the string of the brine withdrawal goes deep into the sediment at the bottom, it is called secondary brine drainage. This paper mainly studies the methods of secondary gas injection and brine drainage. In the progress of secondary brine drainage, the insoluble particles easily plug the brine pipe, causing blockage and affecting the efficiency of brine drainage. Therefore, it is necessary to study sand control technologies in the process of secondary gas injection and brine drainage [32,33].

The advantages and disadvantages of different sand control technologies are shown in Table 4:

**Table 4.** Comparison of sediment control technology characteristics.

Sand Control Technology	Advantages	Disadvantages
Sand control liner [34]	Simple operation and low cost The large inner diameter and strong sand control ability	Not suitable for fine silty sand
Gravel packing technique [35]	High success rate and long validity period The operation effect is not affected by geology	Operation is complicated and the cost is high It is greatly affected by construction parameters
Chemical sand fixation technology [36]	Good effect on fine silt Simple post-processing	High cost, short period of validity Poor temperature adaptability

According to Table 4, the three sand control methods have their own advantages, and there are no direct data based on which to choose the sand control method. Therefore, considering the situation of secondary brine drainage in this block, all three sand control methods are evaluated, which are screen pipe sand control technology, gravel pack artificial well wall sand control technology and chemical sand consolidation technology. In this paper, the sand production pattern of related technologies is presented, and sand control process optimization is gradually carried out.

### 3.1. Experimental Scheme

Gas injection for brine drainage involves injecting natural gas into the chamber after the completion of cave construction. The high-pressure gas squeezes the brine out of the underground. That is, the injection and brine drainage pipe is put into the well, and natural gas is injected into the chamber through injection with high pressure [5,37]. The brine in the chamber is expelled to the ground through the brine drainage pipe. In this paper, the lab experiment design is based on the field sediment to simulate the gas injection and brine drainage procedure. The diagram of gas injection and brine drainage is shown in Figure 5.

In the secondary brine drainage experiment, the brine drainage tube goes deep into the bottom of the salt cavern. Under high pressure, the insoluble particles move to the brine drainage pipe, which can easily cause pipeline blockage [38]. Therefore, it is necessary to evaluate the sand production rules of three kinds of sand control methods, namely, screen pipe, gravel pack artificial well wall and chemical sand consolidation. Figure 6 below shows the simulation diagram of three kinds of sand control technologies.

In order to achieve the simulation of three sand control technologies, the design of secondary brine drainage and the sand control device is as follows:

- (1) According to the actual size of a typical salt cavern gas storage, which has a 160 m height, 50 m diameter and 70 m residue height, the size of the lab simulation experimental device is set as 25 cm in diameter, which is reduced by a factor of 200 in proportion. As the height of the brine drainage pipe is not fixed, a 25 cm height is temporarily used for simulation. The mineral composition and particle size of the particles used are self-made according to the field sediment.
- (2) The experimental process is mainly composed of two parts: one is the secondary gas injection, brine and sand production experiment, and the other is the sand control



experiment. The main purpose of this experiment is to find out the rule of sand production and improve sand control technology. The comparative experiment of each sand control technique is elaborated in Table 4.

- (3) Parameters such as differential pressure, brine layer height and insoluble particle size are considered. The number of insoluble particles and amount of brine production are selected as evaluation criteria.

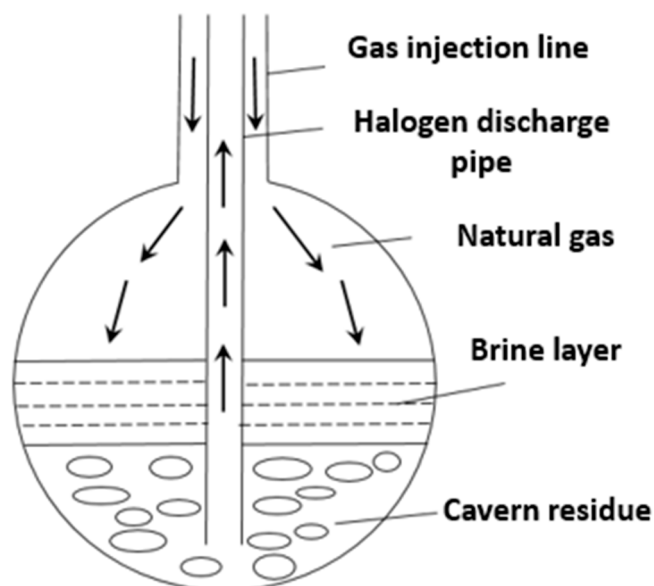


Figure 5. Scheme of secondary gas injection for brine drainage.

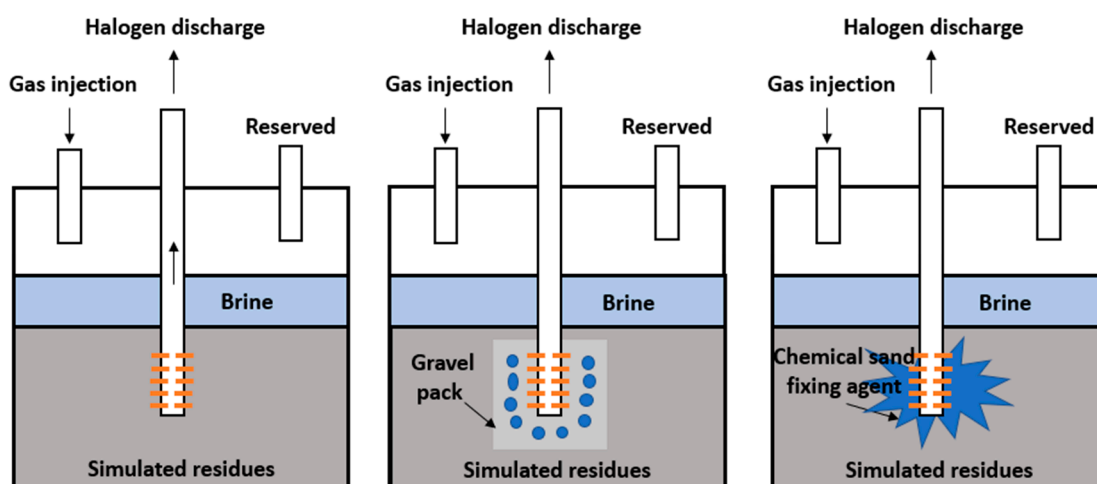


Figure 6. Simulation diagram of three sand control technologies.

### 3.2. Experimental Procedures and Equipment

In order to achieve the simulation of the three sand control technologies, the design rationale of the secondary brine discharge sand control device is as follows: according to the actual size of a typical salt cavern gas storage, which has a 160 m height, 50 m diameter and 70 m residue height, the size of the indoor simulation experimental device in this project is 25 cm in diameter, which is reduced by a factor of 200 in proportion. As the height of the brine discharge pipe is not fixed, a 25 cm high device is temporarily used for simulation. The brine discharge pipe string is reduced by a factor of 14 according to the area, the outer diameter is 8mm, the inner diameter is 6mm and the composition and particle size of the

accumulated materials used are self-configured according to the experimental design and field particle size.

This experiment is a simulation experiment, and the experimental process is as follows: The pressurized gas (0.1–0.2 mpa) is injected into a sealed circular container through the injection pipe, and the injected pressure is recorded. By using different pressures, the brine in the upper container and the pore of insoluble particles is expelled through the brine drainage pipe. The brine drainage time, sand production and brine volume are recorded.

The experimental device includes a high-pressure gas bottle, pressure gauge, cave simulation device, measuring cylinder and timer. Nitrogen is used because it is relatively safer than natural gas. Most of the salt caverns are elliptical, so the experimental device is designed as a cylinder. The brine drainage time is recorded with a stopwatch, the sand production is filtered, dried and weighed by a balance, and the volume of brine is recorded with a measuring cylinder, which is a convenient and fast method. See Figure 7 below.

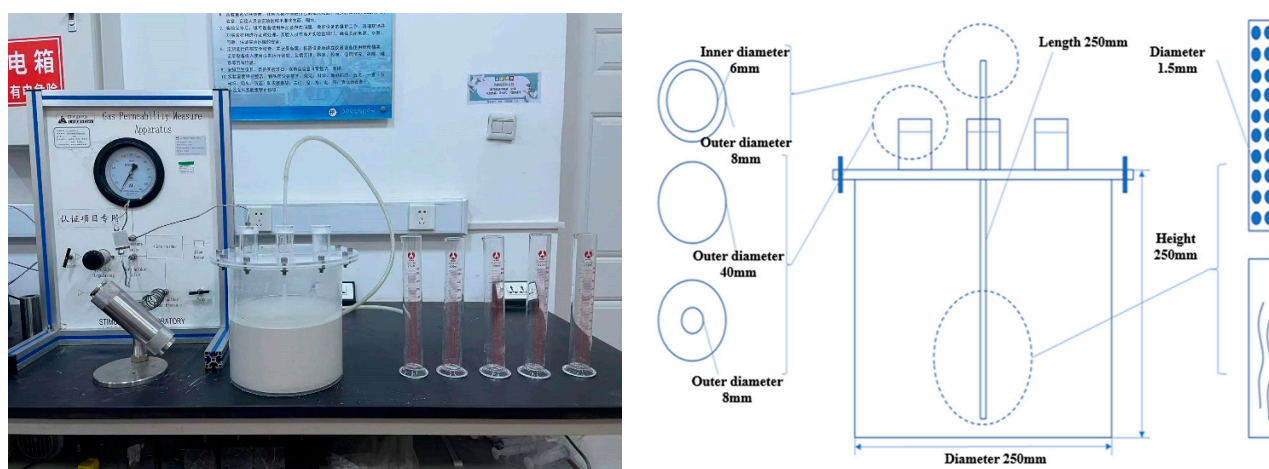


**Figure 7.** Flow chart of experimental device ((Left): physical picture; (Right): schematic diagram).

### 3.3. Experimental Materials

According to the particle size distribution of the sediment from the field, different meshes of quartz with a suitable ratio were used to simulate the sediment at the bottom of the salt cavern. Particle sizes are 100~200 mesh, 200~300 mesh, 300~400 mesh and 400~500 mesh. Furthermore, 100~200 mesh quartz sand is used in artificial well wall sand control experiments, and 25% NaCl solution is used for simulated brine. According to the principle that the grain size of gravel packing is larger than the grain size of formation sand, packing gravel uses quartz sizes of 10~20 mesh, 26~40 mesh and 40~70 mesh.

## 4. Sand Production Rule of Secondary Brine Drainage

In this section, the sand production simulation experiment of secondary gas injection was carried out. A simulation screen with a size 200 times smaller than field conditions was used [39,40]. The acrylic pipe was perforated in advance, with a diameter of 0.15 cm and a total of 40 holes. According to the particle size distribution results obtained in Section 2.1.1. Experimental material, different sizes of quartz are combined according to the ratio from Section 2.2. As shown in Figure 8. We drilled holes spaced 1 cm apart, 3 in a row, for a total of 30 holes.





**Figure 8.** Schematic diagram of brine drainage pipe.

#### 4.1. Effect of Pressure on Brine Drainage and Sand Production

The gas injection pressure was designed to be 0.1 MPa, 0.15 MPa and 0.2 MPa for the experiment. Parameters such as drainage time, drainage volume and quantity of sand production were recorded, and the sand content of the expelled brine was calculated. The experimental results are shown in Figure 9.

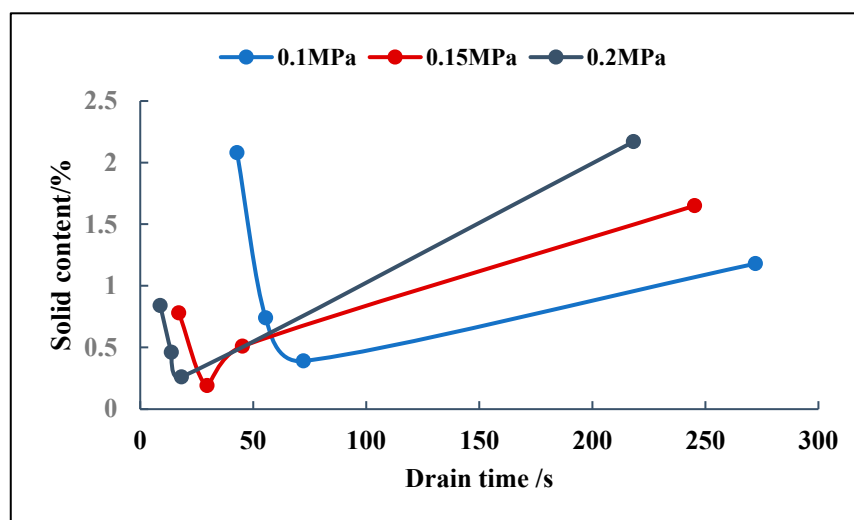


**Figure 9.** The sand content of the expelled brine under different gas injection pressures.

It can be seen from Figure 9 that no matter whether the gas injection pressure is 0.1 MPa, 0.15 MPa or 0.2 MPa, the sand content in expelling brine changes with time in the same mode. When the time is short, the pressure in the chamber is greater than atmospheric pressure due to nitrogen injection, and the loose particles around the brine drainage tube are expelled out of the chamber with the movement of the brine, so the sand content is high. With the change in time, the loose particles are almost expelled, and the remaining sand is compact and difficult to move. At this time, the upper brine is expelled in large quantities due to high pressure, so the content of sand in the brine decreases with the extension of time, showing a downward curve. When the upper brine layer is exhausted, only the brine between the pores of insoluble particles remains in the cavity. Under pressure, this part of brine and gas begins to be expelled quickly at the same time. The gas–liquid mixture drives together the movement of more insoluble particles, and the liquid volume becomes smaller and smaller. Therefore, the sand content began to increase, and the curve showed an upward trend.

By comparing the drainage time when the injection pressure is 0.1 MPa, 0.15 MPa and 0.2 MPa, it can be shown that the injection pressure affects the drainage speed. The

higher the pressure, the faster the drainage speed. However, the total amount of the discharged liquid basically does not change, and the total volume is about 810 mL. The total amount of brine added is about 3500 mL, so about 23.1% of the brine is removed. All three curves showed a descending trend at the beginning and ascending trend at the later stage. With the increase in gas injection pressure, the compaction speed of rock powder is accelerated, which is conducive to reducing the initial sand production amount of rock powder. However, due to the faster gas flow rate in the later gas–liquid discharge, the final sand content also increases. Since the total amount of liquid drainage is basically constant, the total amount of sand production increases under high pressure. According to the experimental results, we believe that sand production can be reduced by reducing the gas-injected pressure. In the following study, the preferred experimental parameter of gas injection pressure is set to 0.1 MPa.

#### 4.2. Brine Layer Height on Brine Drainage and Sand Control

Due to the fact that the brine in the cavern is not drained out after primary gas injection, there is a residual brine layer above the sediment, which is about 2~5 m in height [41]. This experiment aims to explore the influence of the height of the brine layer on sand production. Therefore, the height of the residual brine layer above the sediment is designed to be 2 cm and 4 cm, and the results are shown in Figure 10 below.

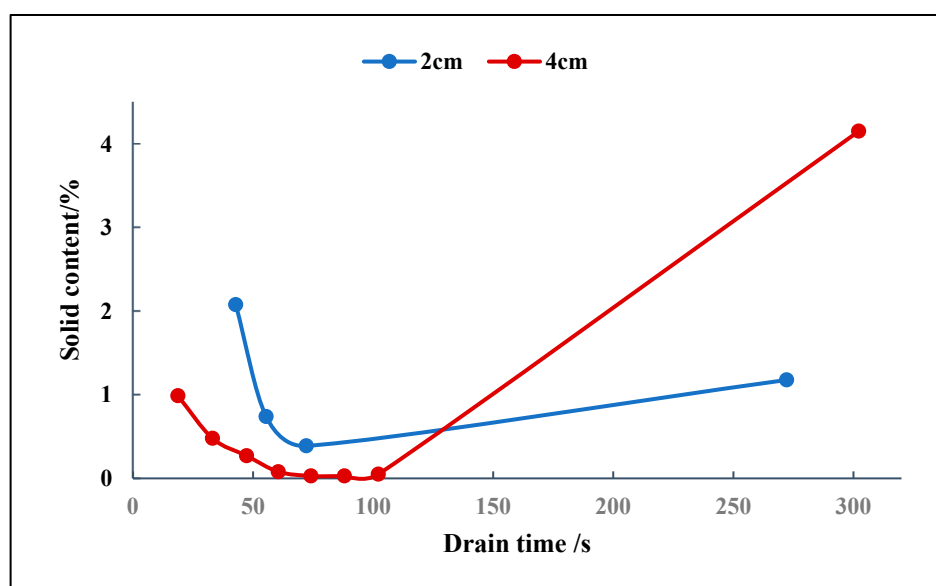


**Figure 10.** Sand content of the expelled brine at different brine layer heights.

When the height of the brine layer increased from 2 cm to 4 cm, the cumulative drainage time increased by a factor of 1.5, and the total amount of sand production was also increased by a factor of about 2. In addition, it can be seen from Figure 10 that when the brine is high in the brine layer, the initial sand production is low but the final sand production is high. However, the trend of the two curves is basically the same. It indicates that the brine layer height does not affect the behavior of brine and sand production. When the height of the brine layer is doubled (4 cm), the liquid discharge time increases by a factor of about 1.5, the liquid drainage volume is about doubled, and the sand content is also about doubled. Therefore, the height of the brine layer does not affect the pattern of the brine drainage. The following experimental parameter of the brine layer height can be set to 2 cm.

#### 4.3. Effect of Particle Sizes on Brine Drainage and Sand Production

The particle size of the sediment at the bottom of the salt cavern is very important for the behavior of brine drainage and sand control. The particle size is not only related to the size of the screen tube but also related to the particle size of the gravel pack. When the insoluble sediment at the bottom of the salt cavern is expelled from the brine pipe, the brine pipe may be blocked, which leads to the impossible removal of the brine and also causes safety problems. Therefore, it is necessary to explore the influence of particle size on the effect of gas injection and brine drainage.

According to the analysis results of the particle size distribution in Section 2.2, the particle sizes of 100–200 mesh, 200–300 mesh, 300–400 mesh and 400–500 mesh were selected for the experiments. The experimental results are shown in Figure 11 below.

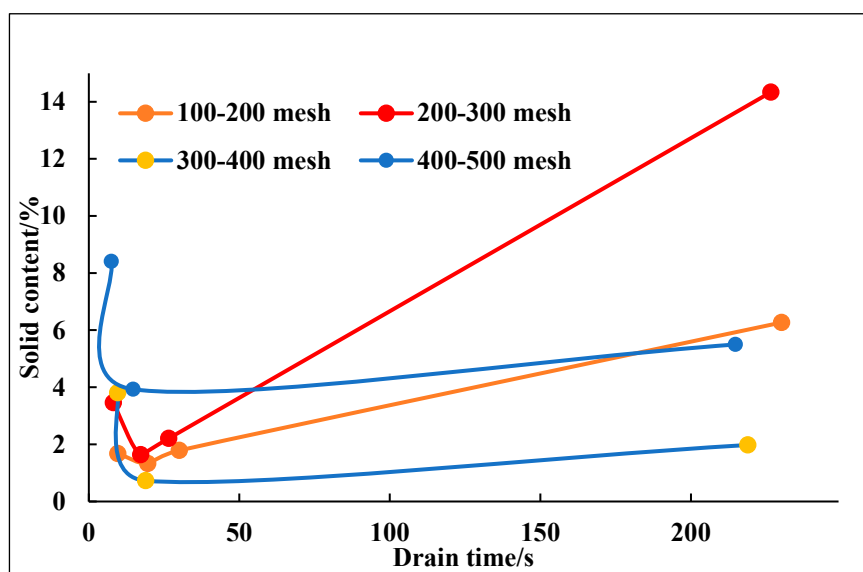


Figure 11. Sand content of the expelled brine at different particle sizes.

It can be seen in Figure 11 that the sand content of the expelled brine with different particle sizes shows a similar trend over time. With the change in time, the loose solid particles were expelled with the brine, and the sand content decreased. The loose particles gradually became compact. When the brine layer is exhausted, the gas–liquid mixture begins to be expelled, and the volume of expelled brine decreases, so the sand content increases again. The four curves show almost the same trend, and there is little relationship between sand production and particle size. It indicates that particle sizes do not affect the sand content of the brine over time obviously.

When the particle size was 100–300 mesh, the sand content increased with the decrease in quartz particle sizes. When the particle size was 300–500 mesh, the sand content increased with the decrease in quartz particle sizes. However, when the particle size was >300 mesh, it can be seen that the sand content of the brine was significantly less than that with a particle size of <300 mesh. The volume of expelled liquid was also significantly reduced. In addition, when the particle size is small, a large number of particles can enter the pipe in the process of brine drainage and cause blockage, which results in the brine in the cavern not being expelled. Therefore, when the particle size is >300 mesh, the effect of brine drainage and sand control is not good. When the particle size is 100 to 300 mesh, the smaller the particle size, the greater the sand content of the expelled brine. The smaller the number of sand mesh, the lower the total amount of brine drainage, which is related to the dense accumulation of fine particles. At the same time, there may be a matching relationship between the mesh number and the hole diameter of the screen. For a 0.15 cm hole, the maximum sand production corresponds to a 300–400 mesh number.

## 5. Sand Control with Gravel Packing and Artificial Well Wall

The conventional gravel packing process is to pack gravel into the formation sand to balance the change in stress caused by the damage to the formation structure and to form a sand control layer for sand control and stabilization. Generally, there is no study on the influence of the thickness of the formed gravel layer on the sand control effect [33]. In this experiment, the artificial well wall and gravel packing process are combined. On the basis of the above screen sand control, gravel is evenly packed outside the perforated brine string so that the packed gravel layer forms an artificial well wall and finally forms the sand control layer. Different gravel particle sizes and different thicknesses of the artificial well wall have different effects on sand control. Therefore, this experiment mainly explores the influence of two factors, that is, gravel size and artificial shaft wall thickness, on the effect of brine drainage and sand control.

### 5.1. Effect of Gravel Size on Brine Drainage and Sand Control

In the artificial well wall experiment, gravel packing with different particle sizes is injected around the brine drainage pipe string to cover the sand control section and isolate the formation sand. Since the particle size of gravel packing is larger than that of formation sand, the formation sand is prevented by gravel packing, which in turn is prevented by the screen pipe string so as to achieve the purpose of sand control. Therefore, the particle size of the gravel pack has a great influence on the sand control effect. This experiment mainly explores the influence of gravel size on brine drainage and sand control. Experiments are first carried out for the same artificial well wall thickness. A size of 100~200 mesh of formation sand is used in this experiment. There is a principle that the gravel size must be larger than the particle size of the formation sand. Therefore, quartz sand with gravel sizes of 10~20 mesh, 26~40 mesh and 40~70 mesh was selected for the experiments. Experimental results are shown in Figure 12.

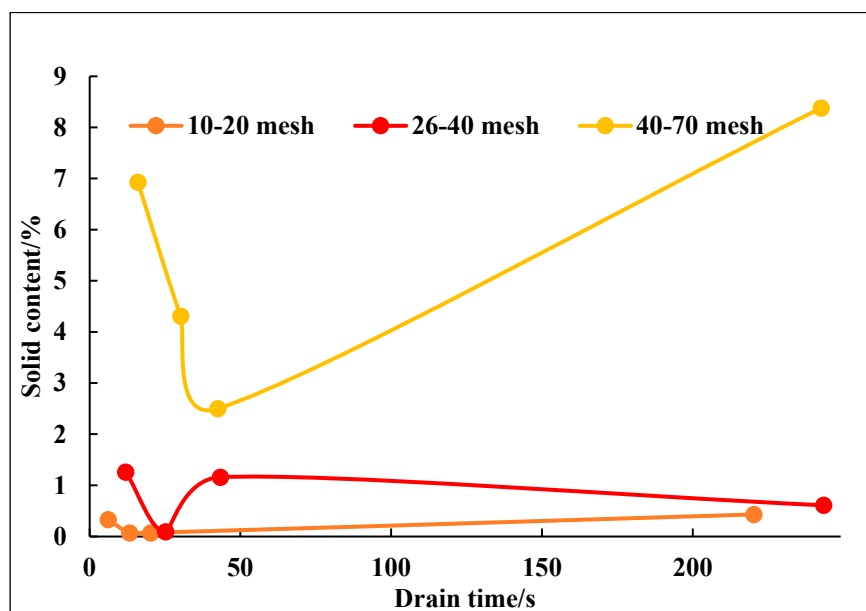


Figure 12. Gravel pack of 1.5 cm thickness with different grain sizes.

When the artificial well wall thickness is constant, the particle size of the gravel pack decreases, and the sand content of expelled brine increases accordingly. Therefore, the smaller the particle size of the gravel pack, the greater the sand content of the brine and the worse the sand control effect of the gravel pack. When the gravel particle size is 10~20 mesh and 26~40 mesh, the sand content of the expelled brine is very low. The total amount of sand production is less than 1 g, and the sand control effect is very good. The

larger the gravel particle size, the lower the sand production. When the gravel particle size is 40~70 mesh, the sand content of the flowback fluid increases sharply, exceeding 10%, and the sand control effect is poor. It may be related to the difficulty in bridging 0.15 cm screen holes under this size. Therefore, according to the results of this experiment, under the condition of the same artificial well wall thickness, the larger the particle size of the gravel pack, the lower the content of solids discharged and the better the sand control effect. When the particle size of the formation sand and gravel converges, the sand production surges, resulting in poor brine drainage and sand control effect.

The curve given in Figure 13 is similar to the sand control effect of a 1.5 cm artificial well wall. The results show that sand production decreases first and then increases with time. The particle size of packing gravel decreases, and the sand content of the flowback brine increases. When the gravel particle size is 10~20 mesh and 26~40 mesh, the sand content of the flowback brine is very low. The total amount is less than 1 g, and the sand control effect is very good. When the gravel particle size is 40~70 mesh, the sand content of the expelled brine increases sharply, exceeding 10%, and the sand control effect is poor. The trend given in Figures 14–16 is similar to the sand control effect of a 1.75 cm artificial well wall.

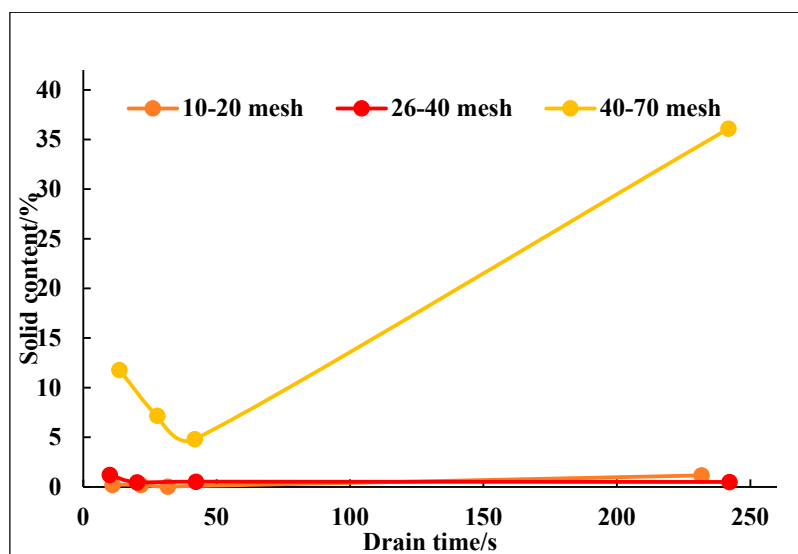


Figure 13. Gravel pack of 1.75 cm thickness with different grain sizes.

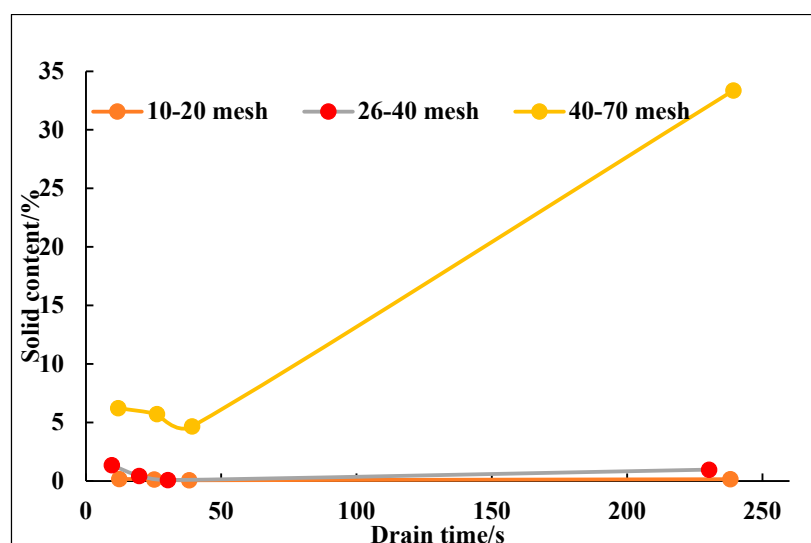


Figure 14. Gravel pack of 2 cm thickness with different grain sizes.

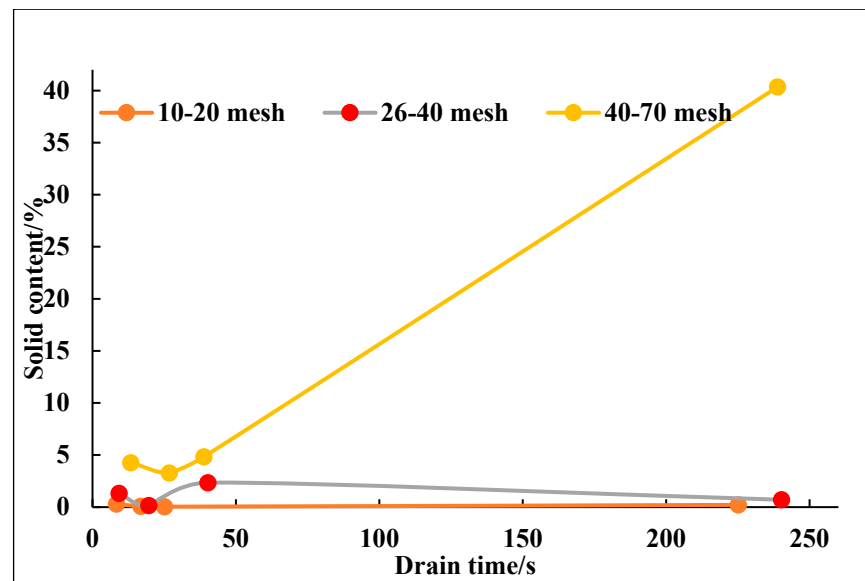


Figure 15. Gravel pack of 2.25 cm thickness with different grain sizes.

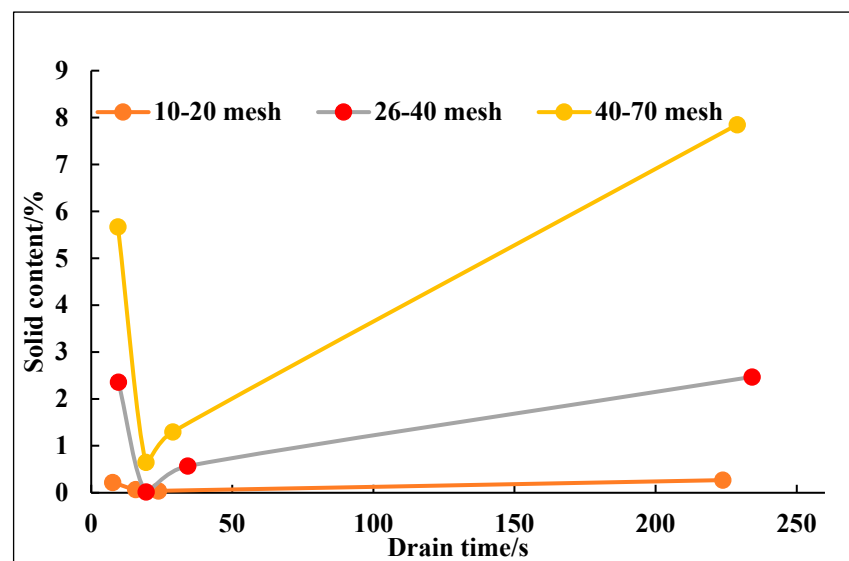


Figure 16. Gravel pack of 2.5 cm thickness with different grain sizes.

### 5.2. Thickness of Artificial Well Wall on Brine Drainage and Sand Control

When the gravel is packed around the brine drainage string, a sand control layer is formed around the pipe, and it is called an artificial well wall. The artificial well wall is between the formation sand and the brine drainage pipe to isolate the formation sand and the screen. The thickness of the artificial well wall has a great influence on the brine drainage and sand control [42]. This experiment mainly explores the influence of different artificial well wall thicknesses on brine drainage and sand control. As previously mentioned, the artificial well wall thickness is designed to be 1.5 cm, 1.75 cm, 2 cm, 2.25 cm and 2.5 cm. The experimental results are shown in Figures 17–20 below.





Figure 17. Effect diagram of brine drainage and sand control.

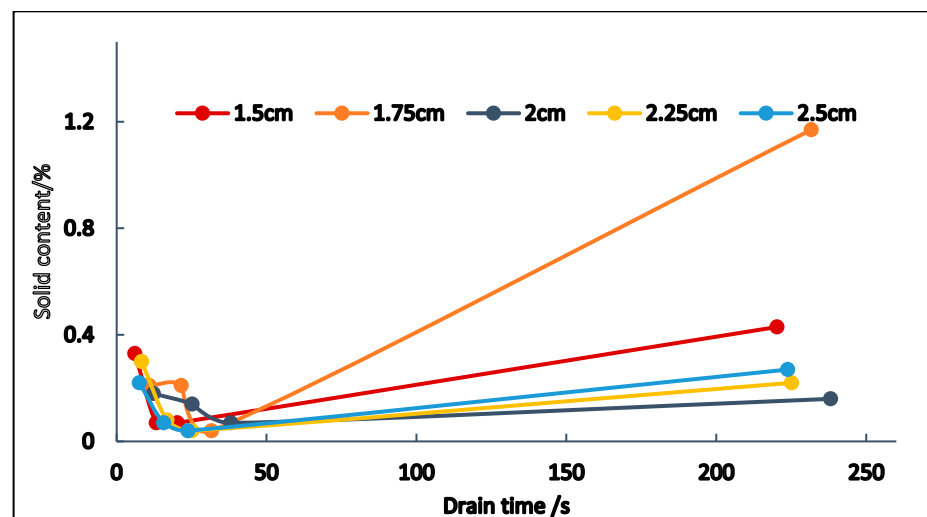


Figure 18. Sand content of the flowback brine with different gravel thicknesses.

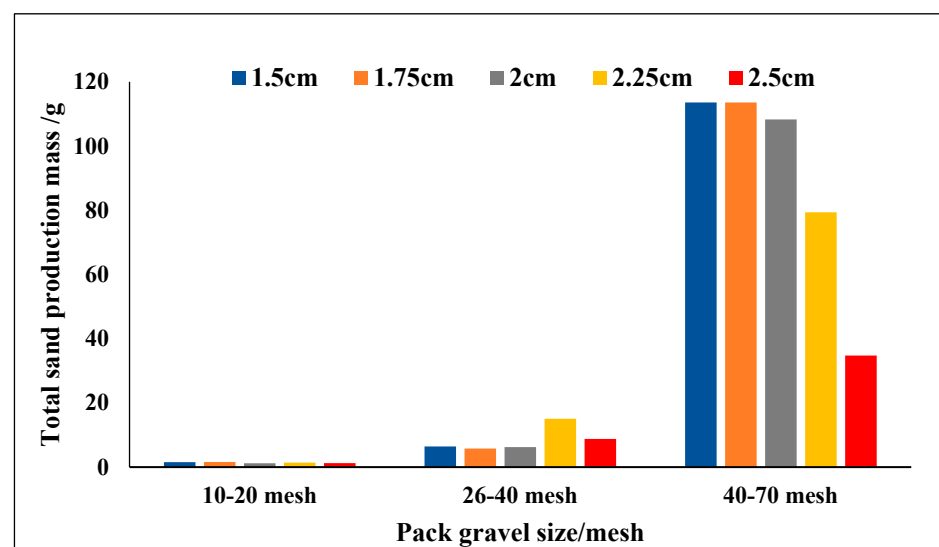
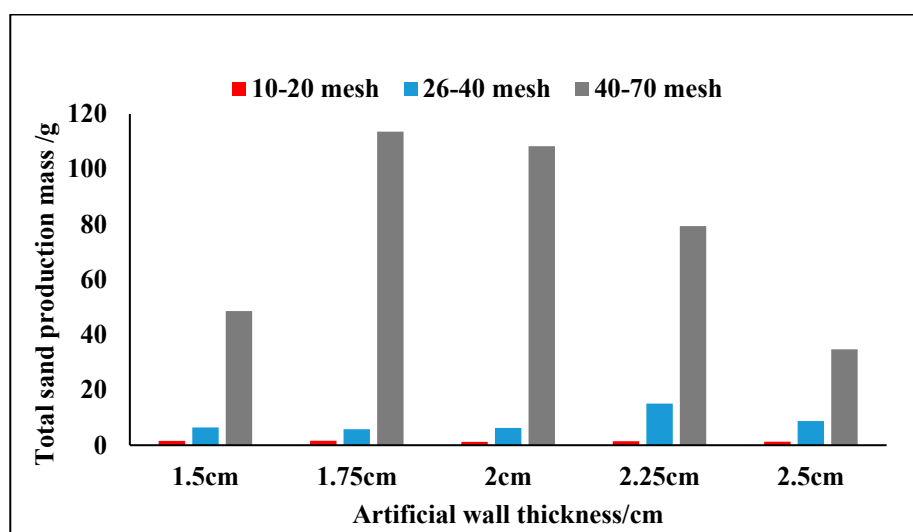


Figure 19. Total sand mass of different filled gravel sizes.



**Figure 20.** Total sand mass at different artificial well walls.

As can be seen from Figures 18–20, under the condition of the same gravel size, the sand content with different artificial well wall thicknesses changes with time basically in the same way, first decreasing and then increasing. Comparing the sand content of the brine, the condition of 40~70 mesh gravel is far greater than that of 26~40 mesh gravel regardless of artificial well wall thickness. The sand production of 26~40 mesh gravel is also significantly greater than that of 10~20 mesh gravel, which again shows that the larger the particle size of the gravel pack, the better the sand control. Under the condition of gravel packing with the same particle size, the trend of sand content with different artificial wall thicknesses is not obvious. The general trend is that the thicker the artificial wall thickness, the better the sand control.

It can be seen from the obtained experimental data that when the thickness of the artificial well wall is 2 cm, the brine drainage and sand control are relatively good. Therefore, sand control is a process controlled by multiple factors. Considering that our model size and field size are 1:200, after conversion, we recommend the best field process as follows: The larger the particle size of the gravel pack, the better the sand control, and the best gravel size is 10–20 mesh. The optimal wall thickness is 2 cm and 28 cm on-site.

## 6. The Evaluation of Chemical Cementing Sand

In the simulation of this experiment, the brine drainage pipe goes deep into the sediment at the bottom of the container, and the chemical adhesive is injected into the sand layer by using high pressure. The sand layer is bonded around the brine drainage pipe that is submerged in the insoluble sediment, which can consolidate to form the sand control layer. This part mainly explores the feature of the chemical sand control process and two kinds of sand adhesives.

Quartz sand with a particle size of 100–200 mesh was selected as simulated sand according to the above experiments. Epoxy resin and phenolic resin were selected as the sand adhesives. The brine is a 25% NaCl solution.

It can be seen from Figure 21 that sand control by different chemical cementing agents shows a similar trend over time. In the beginning, the solid content is high, and with the change in time, the solid content decreases. This is because the brine layer under gas pressure is gradually compacted, and sand production is gradually reduced. When the brine layer is nearly exhausted, the brine in the pores of rock particles is expelled by the gas–brine mixture. The flow rate is faster, the brine production decreases and thus the sand content increases gradually. The two curves almost have the same trend as before.

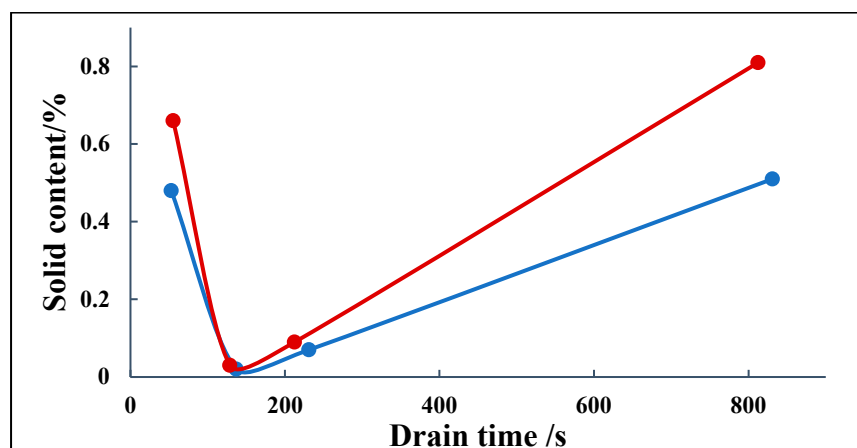


**Figure 21.** Sand content of the expelled brine with two chemical sand cementing agents.

By comparing the drainage time and sand content, it can be shown that the total sand production with two resins is basically the same and is less than 1.0 g, which is comparable to the gravel packing and artificial wall sand control process. However, after epoxy resin cementation, the drainage time is more than 800 s. In the process of gravel packing, this time is about 200~300 s. It indicates that the permeability of the sand body decreased significantly after resin cementation. Therefore, gravel packing is the better sand control technology.

## 7. Conclusions

This paper mainly studies the technology of secondary brine drainage and sand control of unformed rock in salt cavern gas storage. The influence factors and methods of secondary brine drainage and sand control were explored, and the optimal values of each parameter were optimized. The main conclusions are as follows:

- (1) With the increase in gas injection pressure, the sand content of the expelled brine decreases first and then increases, and the total amount of flowback liquid basically remains unchanged.
- (2) The height of the brine layer does not affect the trend of brine drainage and sand production.
- (3) The total brine production increased with the increase in grain size. However, the smaller the particle size, the more difficult the brine in the pores is to expel.
- (4) In the case of artificial wall sand control, the thicker the artificial wall, the larger the gravel size and the better the sand control.
- (5) The two kinds of chemical agents had a good effect on sand consolidation. However, chemical sand control can reduce the permeability of the sand body. Therefore, it is not suitable to be used in salt caverns.
- (6) Under the condition of gravel packing with the same particle size, the trend of sand content with different artificial wall thicknesses is not obvious, and a 2 cm wall thickness is the best in the overall experiment, corresponding to 28 cm in the field. The larger the particle size of the gravel pack, the better the sand control, and the best gravel size is 10-20 mesh.
- (7) Artificial wall sand control has the best sand control effect and a lower sand production rate for uncemented sediments.

**Author Contributions:** Methodology, Y.Z. and K.Z.; software, K.Z.; validation, Y.L. and Y.Z.; investigation, K.Z. and J.L.; data curation, L.-N.R. and Y.Z.; writing—original draft preparation, K.Z. and L.-Q.S.; writing—review and editing, E.-D.Y., Y.Z. and E.-D.Y.; supervision, K.Z.; funding acquisition, E.-D.Y. and K.Z. All authors have read and agreed to the published version of the manuscript.

**Funding:** This research was financially supported by the National Natural Science Foundation of China (grant nos. 52004306 and 52174045), the Strategic Cooperation Technology Projects of CNPC and CUPB (grant nos. ZLZX2020-01 and ZLZX2020-02) and the National Science and Technology Major Projects of China (grant nos. 2016ZX05030005 and 2016ZX05051003).

**Institutional Review Board Statement:** Not applicable.

**Informed Consent Statement:** Not applicable.

**Data Availability Statement:** Not applicable.

**Conflicts of Interest:** The authors declare no conflict of interest.

## References

1. Zhong, M.; Bazilian, M.D. Contours of the Energy Transition: Investment by International Oil and Gas Companies in Renewable Energy. *Electr. J.* **2018**, *31*, 82–91. [CrossRef]
2. Fu, Z.; Chen, Z.; Sharif, A.; Razi, U. The Role of Financial Stress, Oil, Gold and Natural Gas Prices on Clean Energy Stocks: Global Evidence from Extreme Quantile Approach. *Resour. Policy* **2022**, *78*, 102860. [CrossRef]
3. Zhao, K.; Liu, Y.; Li, Y.; Ma, H.; Hou, W.; Yu, C.; Liu, H.; Feng, C.; Yang, C. Feasibility Analysis of Salt Cavern Gas Storage in Extremely Deep Formation: A Case Study in China. *J. Energy Storage* **2022**, *47*, 103649. [CrossRef]
4. Wang, T.; Yan, X.; Yang, H.; Yang, X.; Jiang, T.; Zhao, S. A New Shape Design Method of Salt Cavern Used as Underground Gas Storage. *Appl. Energy* **2013**, *104*, 50–61. [CrossRef]
5. Wanyan, Q.; Ding, G.; Zhao, Y.; Li, K.; Deng, J.; Zheng, Y. Key Technologies for Salt-Cavern Underground Gas Storage Construction and Evaluation and Their Application. *Nat. Gas Ind. B* **2018**, *5*, 623–630. [CrossRef]
6. Li, J.; Wan, J.; Liu, H.; Jurado, M.J.; He, Y.; Yuan, G.; Xia, Y. Stability Analysis of a Typical Salt Cavern Gas Storage in the Jintan Area of China. *Energies* **2022**, *15*, 4167. [CrossRef]
7. Ma, J.; Chen, J.; Chen, W.; Huang, L. A Coupled Thermal-Elastic-Plastic-Damage Model for Concrete Subjected to Dynamic Loading. *Int. J. Plast.* **2022**, *153*, 103279. [CrossRef]
8. Yan, Z.; Wang, Z.; Wu, F.; Lyu, C. Stability Analysis of Pingdingshan Pear-Shaped Multi-Mudstone Interbedded Salt Cavern Gas Storage. *J. Energy Storage* **2022**, *56*, 105963. [CrossRef]
9. Huang, L.; Liang, J.; Ma, J.; Chen, W. A Dynamic Bounding Surface Plasticity Damage Model for Rocks Subjected to High Strain Rates and Confinements. *Int. J. Impact Eng.* **2022**, *168*, 104306. [CrossRef]
10. Juez-Larré, J.; Remmelts, G.; Breunese, J.N.; van Gessel, S.F.; Leeuwenburgh, O. Using Underground Gas Storage to Replace the Swing Capacity of the Giant Natural Gas Field of Groningen in the Netherlands. A Reservoir Performance Feasibility Study. *J. Pet. Sci. Eng.* **2016**, *145*, 34–53. [CrossRef]
11. Jiang, D.; Wang, Y.; Liu, W.; Li, L.; Qiao, W.; Chen, J.; Li, D.; Li, Z.; Fan, J. Construction Simulation of Large-Spacing-Two-Well Salt Cavern with Gas Blanket and Stability Evaluation of Cavern for Gas Storage. *J. Energy Storage* **2022**, *48*, 103932. [CrossRef]
12. Study on the Effect of Fracturing Fluid on the Structure and Mechanical Properties of Igneous Rock. Available online: <https://pubs.acs.org/doi/full/10.1021/acsomega.1c07386> (accessed on 12 February 2023).
13. Yao, E.; Zhang, K.; Wang, Y.; Sheng, L.; Li, Z.; Bai, H.; Zhou, F. Optimization of Shrinkage Agents and Study of Their Shrinking Mechanism for Mudstones in the Salt Cavern Gas Storage. *J. Pet. Sci. Eng.* **2022**, *218*, 110963. [CrossRef]
14. Ma, J.; Wang, J. A Stress-Induced Permeability Evolution Model for Fissured Porous Media. *Rock Mech. Rock Eng.* **2016**, *49*, 477–485. [CrossRef]
15. Yin, H.; Ma, H.; Chen, X.; Shi, X.; Yang, C.; Dusseault, M.B.; Zhang, Y. Synthetic Rock Analogue for Permeability Studies of Rock Salt with Mudstone. *Appl. Sci.* **2017**, *7*, 946. [CrossRef]
16. Luo, Z.; Wang, L.; Yu, P.; Chen, Z. Experimental Study on the Application of an Ionic Liquid as a Shale Inhibitor and Inhibitive Mechanism. *Appl. Clay Sci.* **2017**, *150*, 267–274. [CrossRef]
17. Ning, F.; Fang, X.; Li, Y.; Dou, X.; Wang, L.; Liu, Z.; Luo, Q.; Sun, J.; Zhao, Y.; Zhang, Z.; et al. Research status and perspective on wellbore sand production from hydrate reservoirs. *Bull. Geol. Sci. Technol.* **2020**, *39*, 137–148. [CrossRef]
18. McDowell-Boyer, L.M.; Hunt, J.R.; Sitar, N. Particle Transport through Porous Media. *Water Resour. Res.* **1986**, *22*, 1901–1921. [CrossRef]
19. Hu, X.; Wu, K.; Song, X.; Yu, W.; Tang, J.; Li, G.; Shen, Z. A New Model for Simulating Particle Transport in a Low-Viscosity Fluid for Fluid-Driven Fracturing. *AIChE J.* **2018**, *64*, 3542–3552. [CrossRef]
20. Kulkarni, M.M.; Rao, D.N. Experimental Investigation of Miscible Secondary Gas Injection. In Proceedings of the SPE Annual Technical Conference and Exhibition, Dallas, TX, USA, 9–12 October 2005.
21. Ma, X.; Ding, G. Jintan Complex Layered Salt Rock Gas Storage. In *Handbook of Underground Gas Storages and Technology in China*; Springer: Berlin/Heidelberg, Germany, 2022; pp. 333–375. [CrossRef]
22. Ma, X. Potential Salt Candidates for Storage in Other Parts of China. In *Handbook of Underground Gas Storages and Technology in China*; Springer: Berlin/Heidelberg, Germany, 2022; pp. 895–915. [CrossRef]
23. Bish, D.L.; Post, J.E. (Eds.) *Modern Powder Diffraction*; Walter de Gruyter GmbH & Co KG: Berlin, Germany, 1989; ISBN 978-1-5015-0901-8.

24. Zhang, N.; Shi, X.; Wang, T.; Yang, C.; Liu, W.; Ma, H.; Daemen, J.J.K. Stability and Availability Evaluation of Underground Strategic Petroleum Reserve (SPR) Caverns in Bedded Rock Salt of Jintan, China. *Energy* **2017**, *134*, 504–514. [CrossRef]
25. Li, J.; Shi, X.; Wang, T.; Yang, C.; Li, Y.; Ma, H.; Ma, X.; Shi, H. A Prediction Model of the Accumulation Shape of Insoluble Sediments during the Leaching of Salt Cavern for Gas Storage. *J. Nat. Gas Sci. Eng.* **2016**, *33*, 792–802. [CrossRef]
26. Alabarse, F.G.; Conceição, R.V.; Balzaretto, N.M.; Schenato, F.; Xavier, A.M. In-Situ FTIR Analyses of Bentonite under High-Pressure. *Appl. Clay Sci.* **2011**, *51*, 202–208. [CrossRef]
27. Yu, A.B.; Standish, N. A Study of Particle Size Distributions. *Powder Technol.* **1990**, *62*, 101–118. [CrossRef]
28. Arabkoohsar, A. 1—Classification of Energy Storage Systems. In *Future Grid-Scale Energy Storage Solutions*; Arabkoohsar, A., Ed.; Academic Press: Cambridge, MA, USA, 2023; pp. 1–30. ISBN 978-0-323-90786-6.
29. Research on the Problem of Salt Carried by Gas Injection and Withdrawal of Underground Salt Caverns Gas Storage. U.S. Rock Mechanics/Geomechanics Symposium—OnePetro. Available online: <https://onepetro.org/ARMAUSRMS/proceedings/ARMA21/AII-ARMA21/ARMA-2021-1331/468002> (accessed on 12 February 2023).
30. Wei, X.; Zhichao, Z. Study on the Production Mode and Leakage Risk of Gas Storage Well Completion. *IOP Conf. Ser. Earth Environ. Sci.* **2019**, *233*, 042007. [CrossRef]
31. Lv, Y.T.; Huang, K.; Huang, C.; Fang, L.; Yang, H.J.; Zhang, Z.S.; Luo, S. The Optimization of Injection and Gathering System in Salt Cavern Gas Storage. *Adv. Mater. Res.* **2014**, *1030–1032*, 1366–1369. [CrossRef]
32. Khamsehchi, E.; Ameri, O.; Alizadeh, A. Choosing an Optimum Sand Control Method. *Egypt. J. Pet.* **2015**, *24*, 193–202. [CrossRef]
33. Significant Increase in Sand Control Reliability of Open Hole Gravel Pack Completions in ACG Field—Azerbaijan. SPE European Formation Damage Conference and Exhibition. OnePetro. Available online: <https://onepetro.org/SPEEFDC/proceedings/13EFDC/AII-13EFDC/SPE-165206-MS/177069> (accessed on 26 April 2023).
34. Through-Tubing Sand-Control Techniques Reduce Completion Costs. SPE Drilling & Completion. OnePetro. Available online: <https://onepetro.org/DC/article/9/04/236/69665/Through-Tubing-Sand-Control-Techniques-Reduce> (accessed on 12 February 2023).
35. Parlar, M.; Albino, E.H. Challenges, Accomplishments, and Recent Developments in Gravel Packing. *J. Pet. Technol.* **2000**, *52*, 50–58. [CrossRef]
36. Zang, Y.-X.; Gong, W.; Xie, H.; Liu, B.-L.; Chen, H.-L. Chemical Sand Stabilization: A Review of Material, Mechanism, and Problems. *Environ. Technol. Rev.* **2015**, *4*, 119–132. [CrossRef]
37. Ozarslan, A. Large-Scale Hydrogen Energy Storage in Salt Caverns. *Int. J. Hydrogen Energy* **2012**, *37*, 14265–14277. [CrossRef]
38. Experimental Study on the Performance of Sand Control Screens for Gas Wells. SpringerLink. Available online: <https://link.springer.com/article/10.1007/s13202-012-0019-9> (accessed on 26 April 2023).
39. CFD-DEM Evaluation of Screen Types for Sand Control Applications. *Powder Technol.* **2022**, *404*, 117496. [CrossRef]
40. Screen Selection for Sand Control Based on Laboratory Tests. SPE Asia Pacific Oil and Gas Conference and Exhibition. OnePetro. Available online: <https://onepetro.org/SPEAPOG/proceedings/00APOGCE/AII-00APOGCE/SPE-64398-MS/132284> (accessed on 26 April 2023).
41. Zhang, H.; Wang, P.; Gao, K.; Yue, X. *Study on the Sensitivity of Injection-Production Parameters for the Long-Term Safety and Stability of Salt Cavern Gas Storage*; Research Square: Durham, NC, USA, 2022; in review.
42. Sand Control Techniques—PetroWiki. Available online: [https://petrowiki.spe.org/Sand\\_control\\_techniques](https://petrowiki.spe.org/Sand_control_techniques) (accessed on 26 April 2023).

**Disclaimer/Publisher’s Note:** The statements, opinions and data contained in all publications are solely those of the individual author(s) and contributor(s) and not of MDPI and/or the editor(s). MDPI and/or the editor(s) disclaim responsibility for any injury to people or property resulting from any ideas, methods, instructions or products referred to in the content.